Acta Crystallographica Section D
Biological Crystallography
ISSN 0907-4449

Crystallization and preliminary X-ray diffraction studies of mammalian purple acid phosphatase

Luke W. Guddat,[a]* Alan S. McAlpine,[a] David Hume,[a] John de Jersey,[a] Susan Hamilton[a] and Jennifer L. Martin[b]

[a]Department of Biochemistry, The University of Queensland, St Lucia, Queensland 4072, Australia, and [b]Centre for Drug Design and Development, The University of Queensland, St Lucia, Queensland 4072, Australia

Correspondence e-mail: guddat@biosci.uq.edu.au

Received 8 March 1999
Accepted 4 May 1999

The oxidized form of purple acid phosphatase from pig allantoic fluid has been crystallized in the presence of phosphate using the hanging-drop technique. The crystals belong to the space group $P2_12_12_1$ and have unit-cell parameters a = 66.8, b = 70.3, c = 78.7 Å. Diffraction data collected from a cryocooled crystal using a conventional X-ray source extend to 1.55 Å resolution. A knowledge of the three-dimensional structure of mammalian purple acid phosphatase will aid in understanding the substrate specificity of the enzyme and will be important in the rational design of inhibitors, with potential in the treatment of bone diseases.

1. Introduction

Mammalian purple acid phosphatase (E.C. 3.1.3.2) is a 35 kDa monomeric glycoprotein which catalyses the hydrolysis of a broad range of phosphomonoesters. The enzyme is characterized by a spin-coupled redox-active binuclear Fe^{III}–$Fe^{II/III}$ centre essential for enzymatic activity. The distinctive purple colour of the enzyme results from a charge-transfer transition at 560 nm between a tyrosine and the ferric ion. When the enzyme is reduced to the active Fe^{III}–Fe^{II} form, the charge-transfer band moves to 515 nm, resulting in the protein having a pink colour. To date, no experimental structures of mammalian purple acid phosphatase are available, although the structure of a purple acid phosphatase from red kidney bean has been determined to 2.65 Å resolution (Sträter *et al.*, 1995; Klabunde *et al.*, 1996). Structures of phosphate-bound and tungstate-bound complexes have also been determined to 2.7 and 3.0 Å resolution, respectively (Klabunde *et al.*, 1996). Like mammalian purple acid phosphatase, red kidney bean purple acid phosphatase is a glycoprotein; however, it is a homodimer rather than a monomer and has a much larger subunit molecular weight of 55 kDa. Also in contrast to mammalian purple acid phosphatase, the binuclear centre in the red kidney bean structure is Fe^{III}–Zn^{II} and is not redox active. Based on the red kidney bean crystal structure and a sequence alignment, a tentative model was proposed for the mammalian purple acid phosphatases (Klabunde *et al.*, 1995). In the red kidney bean structure, residues Asp135, Asp146, Tyr167, Asn201, His286, His323 and His325 provide ligands to the metal ions. These residues are completely conserved in the mammalian enzymes, which suggests that the active-site structures in the near vicinity of the metal centre will be very similar. However, the mammalian and plant enzymes share less than 20% sequence identity, indicating that there are likely to be structural differences away from the metal centre. The known mammalian purple acid phosphatases (human, rat, mouse, pig and cow) exhibit sequence identities of 85% or more. Thus, the three-dimensional structure of any of these proteins should provide an excellent model for all the others. We have chosen to study the pig enzyme, also called uteroferrin to highlight its likely role in iron transport from mother to foetus (Schlosnagle *et al.*, 1974; Baumbach *et al.*, 1986). It is present in large quantities in pig allantoic fluid and this is an excellent source for purification (Chen *et al.*, 1973).

Mammalian purple acid phosphatase, of which pig is the best characterized, is also commonly referred to as tartrate-resistant acid phosphatase (TRAP) because, unlike some other mammalian acid phosphatases, it is not inhibited by L-(+)-tartrate. It has also been called type 5 acid phosphatase, based on its electrophoretic mobility. These names reflect the widespread use of this enzyme as a marker for osteoclasts. Experiments with transgenic mice support a role for the enzyme in bone resorption by osteoclasts (Hayman *et al.*, 1996). Inhibitors of human purple acid phosphatase thus have potential as drugs for the treatment of bone diseases such as osteoporosis. The crystal structures of the mammalian enzyme will be critical for the structure-based design of such inhibitors.

2. Materials and methods

2.1. Purification and preparation

Purple acid phosphatase was obtained from the allantoic fluid of 65-day pregnant sows and was purified as described previously (Campbell

Table 1
Data-collection statistics for mammalian purple acid phosphatase.

Temperature (K)	290	100
Resolution range (Å)	50.0–2.00	50.0–1.55
Space group	$P2_12_12_1$	$P2_12_12_1$
Unit-cell parameters (Å)	a = 66.8, b = 70.3, c = 78.7	a = 64.6, b = 70.0, c = 77.1
Mosaicity (°)	0.35	0.68
Crystal size (mm)	0.6 × 0.1 × 0.08	0.8 × 0.15 × 0.10
Number of observations [$I > 0\sigma(I)$]	69826	140370
Unique reflections [$I > 0\sigma(I)$]	24836	46161
R_{sym}† (%)		
Overall	6.4	5.9
Outer shell‡	31.3	27.1
Completeness (%)		
Overall	96.4	89.4
Outer shell‡	94.0	57.4
$I/\sigma(I)$		
Overall	9.4	9.6
Outer shell‡	2.6	2.1

† $R_{sym} = \sum|I - \langle I\rangle|/\sum\langle I\rangle$. ‡ Outer-shell data is in the resolution range 2.07–2.00 Å for data collected at 290 K and 1.61–1.55 Å for data collected at 100 K.

et al., 1978). SDS–PAGE analysis showed that the protein was >95% pure. Dynamic light-scattering experiments using a DynaPro 801 indicated that the protein was monodisperse and, therefore, well suited to crystallization trials (Ferré-D'Amaré & Burley, 1994). Prior to crystallization, the protein was reduced by addition of 58 m*M* ferrous ammonium sulfate and 0.1 *M* β-mercaptoethanol. Addition of excess phosphate led to complete and essentially irreversible oxidation through formation of the oxidized enzyme–phosphate complex (Keough *et al.*, 1982). The specific activity of the reduced protein was 8.05×10^{-6} mol s^{-1} mg^{-1}, while the specific activity after oxidation and in the presence of phosphate was 3.7×10^{-7} mol s^{-1} mg^{-1}.

2.2. Crystallization

Crystals of the oxidized purple acid phosphatase–phosphate complex were obtained by the hanging-drop vapour-diffusion method and a microseeding technique. Initial conditions were found using the sparse-matrix screening approach (Jancarik & Kim, 1991). Clusters of needle-shaped crystals, purple in colour, were produced from a solution which contained equal volumes of well solution *A* [25%(*w*/*v*) PEG 3350, 20%(*v*/*v*) 2-propanol and 0.1 *M* LiCl in 0.1 *M* sodium citrate pH 5.0] and a 38 mg ml^{-1} solution of the oxidized enzyme–phosphate complex. For microseeding, the needle-shaped crystals were crushed into small fragments and the mixture of droplet and crystal fragments was placed in an Eppendorf tube. This solution was then diluted tenfold with well solution *A*. Larger single crystals (Fig. 1) were obtained by streak seeding into a drop which contained equal volumes of well solution *B* [25%(*w*/*v*) PEG 3350, 0.1 *M* LiCl and 5%(*v*/*v*) 2-propanol in 0.1 *M* sodium citrate pH 5.0] and a 38 mg ml^{-1} solution of oxidized enzyme–phosphate complex. After one month, the crystals reached a maximum size of 0.8 × 0.15 × 0.1 mm (Fig. 1).

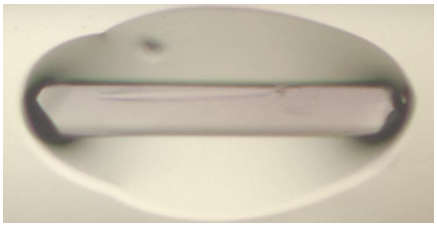

Figure 1
A crystal of mammalian purple acid phosphatase. It is 0.8 mm long and is an intense purple colour, which indicates that the binuclear centre is in the 'inactive' Fe^{III}–Fe^{II} oxidized form.

2.3. Cryocooling and data collection

Crystals were cryoprotected by soaking for 3 min in well solution *B* incorporating 15%(*v*/*v*) glycerol, followed by a further 1 min soak in well solution *B* incorporating 32%(*v*/*v*) glycerol. After this procedure, the crystals were placed directly into the nitrogen stream at 100 K (Oxford Cryosystems Cryostream) for data collection. X-ray diffraction experiments were carried out using a Rigaku RU-200 Cu $K\alpha$ rotating-anode generator (equipped with Yale focusing mirrors) operating at 46 kV and 60 mA. The X-ray diffraction data were recorded on an R-AXIS IIC imaging-plate area detector and were integrated and scaled with the programs *DENZO* and *SCALEPACK* (Otwinowski & Minor, 1997).

3. Results and discussion

Attempts to crystallize this enzyme trace back almost 20 years. The lack of success may have been because of heterogeneity and glycosylation. In the present work, a micro-heterogeneity problem resulting from the possible coexistence of several enzyme forms in solution (reduced, oxidized, phosphate complexes, apoproteins) has been eliminated by converting the enzyme to a single molecular form, the very stable oxidized enzyme–phosphate complex. The formation of a single species prior to crystallization could be important for diffraction quality. For example, a report from 1994 of small needle-like crystals (0.25 × 0.05 × <0.05 mm) of human purple acid phosphatase (Hayman & Cox, 1994) provided no details of diffraction data quality and has not yet yielded a published crystal structure.

Preliminary analysis of our crystals at room temperature showed that they belonged to the space group $P2_12_12_1$ with unit-cell parameters a = 66.8, b = 70.3, c = 78.7 Å. Initially, crystals diffracted strongly to better than 2.00 Å resolution, but after 18 h of exposure to X-rays the intensity of reflections had decreased by more than 66%. Therefore, it was necessary to develop a cryocooling strategy to minimize crystal radiation damage. The cryocooled crystals have slightly contracted unit-cell parameters, a = 64.6, b = 70.0, c = 77.1 Å. Based on one protein molecule per asymmetric unit, the solvent content for the cryocooled crystals is calculated to be 51% (V_m = 2.3 Å^3 Da^{-1}), compared with 54% for the room-temperature crystals. These values are within the expected range for proteins (Matthews, 1968). Data-collection statistics are summarized in Table 1. Attempts to solve the structure by molecular replacement using the C-terminal domain of the red kidney bean enzyme have not been successful. Consequently, the techniques of multiple isomorphous replacement (MIR) or multiwavelength anomalous diffraction (MAD) will be investigated to solve the phase problem. Several promising heavy-atom derivatives for MIR have already been identified. The high-resolution diffraction data from the measured cryocooled crystals should enable determination of a very accurate structure for mammalian purple acid phosphatase, which will be an important factor in the future success of structure-based drug-design studies.

This work was supported by a grant-in-aid from Johnson and Johnson Research Pty Ltd and by the Australian National Health and Medical Research Council. JLM was the recipient of an ARC Queen Elizabeth II Fellowship.

References

Baumbach, G. A., Ketcham, C. M., Richardson, D. E., Bazer, F. W. & Roberts, R. M. (1986). *J. Biol. Chem.* **261**, 12869–12878.

Chen, T. T., Bazer, F. W., Cetorelli, J. J., Pollard, W. E. & Roberts, R. M. (1973). *J. Biol. Chem.* **248**, 8560–8566.
Campbell, H. D., Dionysius, D. A., Keough, D. T., Wilson, B. E., de Jersey, J. & Zerner, B. (1978). *Biochem. Biophys. Res. Commun.* **82**, 615–620.
Ferré-D'Amaré, A. R. & Burley, S. K. (1994). *Structure*, **2**, 357–359.
Hayman, A. R. & Cox, T. M. (1994). *J. Biol. Chem.* **269**, 1294–1300.
Hayman, A. R., Jones, S. J., Boyde, A., Foster, D., Colledge, W. H., Carlton, M. B., Evans, M. J. & Cox, T. M. (1996). *Development*, **122**, 3151–3162.
Jancarik, J. & Kim, S.-H. (1991). *J. Appl. Cryst.* **24**, 409–411.
Keough, D. T., Beck, J. L., de Jersey, J. & Zerner, B. (1982). *Biochem. Biophys. Res. Commun.* **108**, 1643–1648.
Klabunde, T., Sträter, N., Fröhlich, R., Witzel, H. & Krebs, B. (1996). *J. Mol. Biol.* **259**, 737–748.
Klabunde, T. Sträter, N., Krebs, B. & Witzel, H. (1995). *FEBS Lett.* **367**, 56–60.
Matthews, B. M. (1968). *J. Mol. Biol.* **33**, 491–497.
Otwinowski, Z. & Minor, W. (1997). *Methods Enzymol.* **276**, 307–326.
Schlosnagle, D. C., Bazer, F. W., Tsibris, J. C. M. & Roberts, R. M. (1974). *J. Biol. Chem.* **249**, 7574–7579.
Sträter, N., Klabunde, T., Tucker, P., Witzel, H. & Krebs, B. (1995). *Science*, **268**, 1489–1492.